

Green Chemistry

Accepted Manuscript



This article can be cited before page numbers have been issued, to do this please use: P. Caramazana, P. Dunne, M. Gimeno-Fabra, M. Zilka, M. Ticha, B. Stieberova, F. Freiberg, J. McKechnie and E. Lester, *Green Chem.*, 2017, DOI: 10.1039/C6GC03357A.



This is an Accepted Manuscript, which has been through the Royal Society of Chemistry peer review process and has been accepted for publication.

Accepted Manuscripts are published online shortly after acceptance, before technical editing, formatting and proof reading. Using this free service, authors can make their results available to the community, in citable form, before we publish the edited article. We will replace this Accepted Manuscript with the edited and formatted Advance Article as soon as it is available.

You can find more information about Accepted Manuscripts in the [author guidelines](#).

Please note that technical editing may introduce minor changes to the text and/or graphics, which may alter content. The journal's standard [Terms & Conditions](#) and the ethical guidelines, outlined in our [author and reviewer resource centre](#), still apply. In no event shall the Royal Society of Chemistry be held responsible for any errors or omissions in this Accepted Manuscript or any consequences arising from the use of any information it contains.



Journal Name

ARTICLE

Assessing the life cycle environmental impacts of titania nanoparticle production by continuous flow solvo/hydrothermal synthesis

P. Caramazana-González,^a P. W. Dunne,^{a,b} M. Gimeno-Fabra,^a Miroslav Zilka^c, M. Ticha^c, B. Stieberova^c, F. Freiberg^c, J. McKechnie^a and E. H. Lester^a

Received 00th January 20xx,
Accepted 00th January 20xx

DOI: 10.1039/x0xx00000x

www.rsc.org/

Continuous-flow hydrothermal and solvothermal synthesis offer substantial advantages over conventional processes, producing high quality material from a wide range of precursors. In this study, we evaluate “cradle-to-gate” life cycle environmental impacts of alternative titanium dioxide (TiO₂) nanoparticle production parameters, considering a range of operational conditions, precursors, materials properties and production capacities. Detailed characterisation of the nano-TiO₂ products allows us, for the first time, to link key nanoparticle characteristics to production parameters and environmental impacts, providing a useful foundation for future studies evaluating nano-TiO₂ applications. Five different titanium precursors are considered, ranging from simple inorganic precursors, like titanium oxysulphate (TiOS), to complex organic precursors such as titanium bis(ammonium-lactato) dihydroxide (TiBALD). Synthesis at laboratory scale is used to determine yield, size distribution, crystallinity and phase of the nanoparticles. Specifications and operating experience of a full scale plant (>1000 t/yr) are used to estimate mass and energy inputs of industrial scale production for the life cycle assessment. Overall, higher process temperatures are linked to larger, more crystalline nanoparticles and higher conversion rates. Precursor selection also influences nano-TiO₂ properties: production from TiOS results in the largest particle sizes, while TiBALD achieves the smallest particles and narrowest size distribution. Precursor selection is the main factor in determining cradle-to-gate environmental impacts (>80% in some cases), due to the production impacts of complex organic precursors. Nano-TiO₂ production from TiOS shows the lowest global warming potential (GWP) (< 12 kg CO₂-eq/kg TiO₂) and cumulative energy demand (CED) (<149 MJ/kg TiO₂) due to the low environmental impact of the precursor, the use of water as a solvent and its high yield even at lower temperatures. Conversely, the TiBALD precursor shows the highest impacts (86 kg CO₂-eq/kg TiO₂ and 1952 MJ/kg TiO₂), due to the need for additional post-synthesis steps and complexity of the precursor manufacturing. The main purpose of this study is not a direct comparison of the environmental impacts of TiO₂ nanoparticles manufactured utilizing various precursors under different conditions, but to provide an essential foundation for future work evaluating potential applications of nano-TiO₂ and their life cycle environmental impacts.

1. Introduction

1.1 TiO₂ production methods

Titanium dioxide or titania (TiO₂) is one of the most widely used and studied materials due to its chemical and physical properties, including high thermal and chemical stability,¹ high refractive index, non-toxicity, high hardness, catalytic and photocatalytic activity.^{2,3} It is used in medical implants,⁴ water

purification,⁵ pigments in the paper and paints industries,⁶ plastics and fibres.² Industrial processes have been improved since early last century making TiO₂ production one of the most commoditised materials in the chemicals industry. However alternative routes, capable of producing nano-sized TiO₂, have gained interest in the recent years e.g. sol-gel⁴ spinning disk⁷ solvothermal and hydrothermal synthesis.^{8,9} have been developed to produce nanoparticles of titanium dioxide. With the increase in awareness of environmental concerns it is ever more important to address the potential environmental impact of industrial processes, both current and emerging.

1.2 Spectrum of precursors used for TiO₂ synthesis

The sulphate process was the first method to produce titania as a pigment for different paints. In the 1950s, the production increased and the chloride process appeared as an

^a Advanced Materials Research Group, Faculty of Engineering, University of Nottingham, Nottingham, NG7 2RD.

^b School of Chemistry, Trinity College, College Green, Dublin 2, Ireland.

^c Czech Technical University in Prague, Faculty of Mechanical Engineering, Department of Enterprise Management and Economics, Prague, Czech Republic.

† Footnotes relating to the title and/or authors should appear here.

Electronic Supplementary Information (ESI) available: [details of any supplementary information available should be included here]. See DOI: 10.1039/x0xx00000x

alternative.¹⁰ Unlike these traditional processes, new methods developed in the last years (sol-gel, solvothermal and hydrothermal) possess better advantages to control of phase, size, shape and composition.¹ Despite these significant benefits, these techniques are typically batch processes with poor scope for scale-up. Continuous-flow hydrothermal synthesis (CFHS) was developed by Adschiri *et al.*^{11,12} as a new synthesis of metal oxide nanoparticles. Continuous-flow solvothermal synthesis (CFSS) has also been shown to produce a larger variety of more complex nanomaterials such as metal-organics framework (MOFs).^{9, 13, 14} As continuous methods CFHS and CFSS are inherently more scalable than conventional batch synthesis. This technique exploits the properties of superheated water – its high dissociation constant and low polarity – to nucleate metal oxide nanocrystals on mixing a stream of metal salt solution with a superheated water stream. Early work in this field used a simple, off-the-shelf “tee reactor”. Later, Lester *et al.*¹⁵ designed a new reactor for CFHS and CFSS, known as a “nozzle” or counter-current reactor, taking advantage of the low density of supercritical water to achieve symmetric mixing and a narrow residence time distribution. This reactor has been demonstrated at a wide range of different conditions (temperature, solvents, precursors, etc.), offering an easy and reproducible process, as well as the capacity to producing many materials with distinct shapes and sizes¹⁴⁻²³. The nozzle reactor has also achieved the continuous production of nanoparticles from laboratory scale to pilot scale to full scale.²⁴ By all of these advantages (reproducibility, scalability, flexibility and potential as an environmentally benign process), CFHS and CFSS stand to play important role in the large-scale production of nanomaterials. CFHS and CFSS methods have used a wide range of titanium precursors, with both organic and inorganic components, for the production of nanoparticles of TiO₂.^{8, 9, 25-30} Titanium tetrachloride (TiCl₄) as a halide salt can be easily hydrolysed¹ to produce TiO₂ with water.^{25, 26} Titanium oxysulfate, or titanyl sulphate (TiOS), which is an intermediate product from the sulphate process,² can also be synthesised in a continuous system with an aqueous flow.²⁸ Alkoxides (Ti(OR)₄), such as titanium isopropoxide (TIPO) are frequently used in non-aqueous sol-gel methods due to their sensitivity to water,^{31, 32} as well as, in CFSS with solvents such as butanol or isopropanol.^{9, 27, 30} Water-soluble titanium complexes (WSTC) are derivatives of TiCl₄ or TIPO with an acid such as glycolic, lactic, oxalic, etc. and a base like ammonia (NH₃) or potassium hydroxide (KOH).^{33, 34} Titanium bis(ammonium lactato) dihydroxide (TiBALD), is one of the WSTC precursors that has already been able to produce nano-TiO₂ at pilot-plant scale (kg's/day) by CFHS.²⁹ Unlike the alkoxides and TiCl₄, these complexes are stable in water,³⁵ permitting their use in aqueous reaction systems. The main difference between precursors is the degree of manufacturing. Inorganic precursors like TiOS and TiCl₄ are easily produced by mixing the mineral (raw material) with an acid solution. Alkoxide and WSTC are more complex precursors (and subsequently more expensive), but with a higher stability due to the interaction of the organic counter ion around the titanium atom.

1.3 Overview of TiO₂ LCA studies

The increased industrial scale use of CFHS and CFSS for production of large quantities of nanoparticles necessitates a thorough assessment of environmental sustainability of this newly developed process. For this purpose, a standardised method Life Cycle Assessment (LCA) was used as a tool for quantification of the potential environmental impacts of a product system throughout its life cycle. Prior LCA studies have evaluated TiO₂ production from “cradle-to-gate” (excluding the application, product use and end-of-life of nano-TiO₂), including traditional and new techniques at different scales and size of TiO₂ particles. Reck *et al.*¹⁰ compared between traditional industries (sulphate and chloride) with different feedstocks and waste treatments. This study was based on energy requirements, sulphur oxides emissions, solid waste and metal discharge into the water as environmental factors, concluding that sulphate process (ilmenite) demands less energy but generates more residue and emissions than the chlorine process (slag or rutile). Unlike of traditional methods, the Altair Hydrochloride process (AHP) produces nano-TiO₂ using ilmenite and hydrochloric acid. Grubb *et al.*⁶ calculated the energetic demand for the AHP; deducing that energy consumed is similar to sulphate process, despite the fact that AHP is able to produce nano-TiO₂. Middlemas *et al.*³⁶ carried out a LCA study for the process known as Alkaline Roast of Titania Slag (ARTS)³⁷. This alternative route uses titanium slag and sodium hydroxide to produce micro-titania particles of 0.2-0.3 μm. The emissions of CO₂ and the cumulative energy demand (CED) were used as impact factors. Middlemas *et al.* compared the results with other LCA studies concluding ARTS process emits less CO₂ and demands less energy than the traditional processes and the Altair method. A “cradle-to-gate” LCA was also carried out for the hydrolytic synthesis of TiO₂ nanoparticles.³⁸ TIPO and water were used in a sol-gel synthesis to get a suspension of nanoparticles at 6% wt. and 30 nm of size. The LCA results determined that the most impacts are produced by the high demand of energy required for operating the process including temperature, as well as the use of an organic precursor with higher environmental impacts as TIPO. The focus of prior studies on single combinations of titanium precursor and production parameters and the lack of detailed nano-TiO₂ characterisation data presented in these studies i) provides limited insights regarding the impact of precursor and process parameters on environmental impact; ii) prevents useful inter-study comparisons and iii) raises questions as to the functional equivalence of the evaluated materials and their suitability for specific end uses. In this article, we evaluate the technical performance and environmental impacts of continuous-flow solvo-hydrothermal synthesis of nano-TiO₂. A broad set of titania precursors are considered to characterise the nano-TiO₂ in terms of size distribution, crystallinity, phase and yield at laboratory scale. This experimental data are extrapolated to assess the environmental impacts of commercial scale production based on operational experience, primary data from units, mass and energy balance of a facility (> 1000 ton/year).³⁹

2. Methods

The environmental assessment for the synthesis of TiO₂ nanoparticles was carried out in a set of temperatures 250–400 °C and precursors. It was modelling using the LCA methods,^{40, 41} laboratory work for the synthesis of TiO₂ nanoparticles, literature review and information from the EU funded SHYMAN industrial plant (www.shyman.eu). All of this information is detailed in this section.

2.1 Scope and Goal

Life cycle assessment models were developed to quantify environmental impacts associated with industrial-scale nano-TiO₂ production using five different precursors at five different temperatures. This means that 25 potential variants of the industrial process were assessed in this study. A “cradle-to-gate” scope of LCA was chosen. The system boundary encompassed all inputs and outputs from raw material excavation for production of precursors, process chemicals and energy including transportation and all processes for nano-TiO₂ production. Given the diverse uses of nano-TiO₂, we did not consider a specific use in the present study. Mass and energy balances of nano-TiO₂ production, based on experimental investigations for each precursor and temperature combination at laboratory scale and specifications of the industrial facility, were used as inputs to the life cycle inventory (LCI). LCA results were calculated in SimaPro 8.0.4, using the necessary databases (e.g. Ecoinvent 3 database v.3). In the cases where the information was unknown, literature sources were used alongside and chemical simulation engineering software (Aspen Hysys V8.4). Transportation of all precursors was taken into account, considering an average of 200 km. Packaging of the precursor was defined according to the specifications of suppliers. Due to a scope of the system from cradle-to-gate the final product that leaves the system boundaries is an aqueous suspension with different concentrations of nanoparticles. For this reason, a declared unit (instead of functional unit) was established and was determined as 1 kg nano-TiO₂. Environmental impacts were calculated in two impact categories - cumulative energy demand (CED) and global warming potential (GWP). CED is expressed in megajoules per kilogram of product (MJ/kg). GWP was estimated in kilograms of CO₂-equivalent per kilogram of product (CO₂-eq/kg), based on the 100-year global warming potential of greenhouse gas (GHG) emissions.

2.2 Precursors Manufacturing

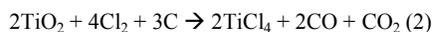
TiOS and TiCl₄ were chosen as they are the most basic inorganic precursor salts. Titanium isopropoxide (TIPO), TiBALD and Potassium titanium oxide oxalate dehydrate (PTOOD) were selected as organic alternatives. Information about the production of precursors is limited, and, as such, the literature was reviewed to determine the processes of production for the five precursors studied. The production methods of the precursors are described here, while a scheme of production and mass and energy inputs table are provided in the Supporting Information (SI).

TiOS, can be obtained from the industrial sulphate process for TiO₂ production. The process uses ilmenite or slag as raw materials commonly, and these are digested in an exothermic reaction:



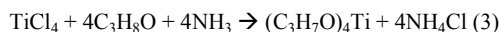
The reaction uses an excess of acid between 1.5–1.7 times the mass requirement.³ The yield of titanium is about 95%. When ilmenite is used as raw material, it is necessary to add scrap iron to reduce any ferric iron to ferrous. After digestion the solution passes different separation methods (filtration and decantation) to remove iron and other impurities.¹⁰ Literature review detailed the materials inputs.^{10, 42} Electricity and natural gas inputs for the production 1kg of TiOS was evaluated using Aspen Hysys V8.4 software (UNIQUAC property package).

TiCl₄ is an intermediate product of the chloride process, which generally uses rutile deposits as raw material. Mineral rutile has a higher percentage of TiO₂ content (90–98%) than ilmenite ores,² and thus the chloride process produces less waste than sulphate method. Firstly, the raw materials (coke, chlorine and rutile) are mixed in a fluidised-bed reactor. The exothermic reaction is maintained at 950 °C. The reaction is:



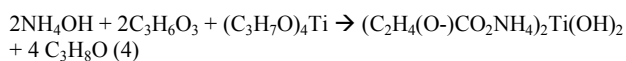
After chlorination, many of the impurities and chlorinated metals are removed as solid residue. Finally, the gas stream is cooled and the liquid is distilled to form TiCl₄ as the final product.² Production and purification of TiCl₄ were simulated in Aspen Hysys V8.4 (UNIQUAC property package) according to the literature^{43, 44} to a defined mass and energy balance, operating at steady state.

Unfortunately, information about production of TIPO is quite scarce. One of the first methods to produce TIPO was developed by Johannes Nelles in 1940.⁴⁵ Later in 1952, a similar process was described by Bradley *et al.*^{46, 47}



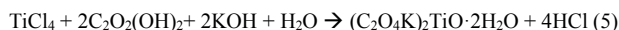
According to literature the yield is between 72 and 80%.^{47, 48} Benzene is used to precipitate the NH₄Cl.⁴⁵ The quantity of benzene is not specified, so it was assumed to be a volume equal to the volume of mixture of 2-propanol (IPA) and TiCl₄. The recovery of benzene and IPA was simulated in Aspen Hysys V8.4 (UNIQUAC property package) to quantify the energy used during the separation process.

TiBALD was synthesized with TIPO, lactic acid and aqueous ammonia solution in water by Ohya *et al.*³³ Firstly, both TIPO and lactic acid are mixed at a ratio of 1:2. The addition of water results in a precipitate which re-dissolves under stirring. Finally, ammonia is added, such that the full process can be described as:



According to literature the yield is 80%.⁴⁸ The energy of stirring was estimated establishing a relation volume between an

industrial stirring system (1 hour stirring 500 litres is 0.25 kW) and the solution volume. The distillation to recover the IPA was simulated by Aspen Hysys V8.4 (NTRL property package). PTOOD was synthesised in a similar way to TIPO. TiCl_4 , oxalic acid, potassium hydroxide and water were used by Brisse *et al.*³⁴ Firstly, aqueous solutions of TiCl_4 and oxalic acid are mixed, followed by the slow addition of potassium hydroxide. With the formed complex precipitated by the addition of ethanol:



The reactants were adjusted at equimolar values for in the mass balance. Oxalic acid inputs production was defined according to Sullivan *et al.*⁴⁹ Ethanol distillation and cooling system were simulated in Aspen Hysys V8.4 (UNIQUAC property package), while stirring stages were calculated as previously mentioned.

2.3 Laboratory synthesis

Five different precursors were selected to synthesise nano- TiO_2 nanoparticles with the nozzle reactor:

- TiOS: Titanium (IV) oxysulfate (99.99%) 15% wt. in dilute sulphuric acid
- TiCl_4 : Titanium (IV) chloride (99.9%)
- TIPO: Titanium (IV) isopropoxide (97%)
- TiBALD: Titanium (IV) bis(ammonium lactato) dihydroxide solution (50%wt in H_2O)
- PTOOD: Potassium titanium oxide oxalate dehydrate powder (98%)

All precursors were supplied by Sigma Aldrich and used as received. Deionised water (10 M Ω) and 2-Propanol (99.5%), also from Sigma Aldrich, were used as solvents.

A schematic of the reactor used is presented in Figure 1. The reactor has been described in detail elsewhere.¹⁵ Briefly, it is comprised of a preheater section which feeds a heated stream downwards (the downflow) through an inner tube into a vertically aligned outer tube through which room temperature precursor streams are pumped (upflow). The heated and precursor streams mix at the outlet of the inner tube before immediately passing through a heat exchanger to cool down. All fittings and tubing are stainless steel 316L Swagelok® parts. The product stream exits through a back pressure regulator which maintains pressure within the system. The heated downflow and the precursor streams are delivered into the system via HPLC pumps.

Certain precursors are unstable in water which means that alternative solvents are needed in the upflow. 0.05 M solutions of each precursor were prepared:

- TiOS + Deionised water
- TiCl_4 + 2-Propanol
- TIPO + 2-Propanol
- TiBALD + Deionised water
- PTOOD + Deionised water

Deionised water was used as the heated downflow for the production of titanium dioxide when solutions A, B and C were pumped as metal salts. For solutions D and E, the hot stream

was a solution of water with a 5 volume % solution of hydrogen peroxide (H_2O_2 , 1.108g/ml, 100 volumes 30% supplied by Fisher Scientific) to ensure the decomposition of the organic components of the WSTC precursors.

The pressure of system was established at 240 bar, while that the temperature for the reaction was varied from 200 °C to 400 °C at increments of 50 °C, such that, product was collected for five different temperatures for each precursor (200, 250, 300, 350 and 400 °C). The flows were consistent for each reaction at 20 ml min⁻¹ for the downflow and 10 ml min⁻¹ for the precursor stream.

Samples of known volume were centrifuged at 4000 rpm for 5 minutes to separate nanoparticles and liquid from the initial suspension. Some samples required the addition of a precipitant (nitric acid) to promote sedimentation before centrifugation (see Table 1), probably due to organics radicals stabilising the suspensions. The obtained solids were dried in an oven for 24 h at 70 °C before weighing and further characterisation. The mass of solid obtained from known volumes of the product suspension gave a crude yield.

2.4 Characterisation

X-ray powder diffraction (XRD) patterns were collected on a Bruker AXS D8 Advance X-ray diffractometer with Cu K α radiation ($\lambda = 0.15418$ nm) across a 2θ range of 15–65° with an step size of 0.04° at a collection time of 5 s/step. Crystallite diameters were calculated using the Scherrer equation from the FWHM determined by profile fitting with Xfit. Samples were prepared for transmission electron microscopy (TEM) by resuspending a small quantity of dried powder in acetone and depositing it onto lacey carbon coated copper grids (300 mesh). TEM images were obtained using a JEOL 2100F high resolution TEM at an accelerating voltage of 200 kV. Particle size distributions were measured using ImageJ® using a previously described approach.²¹ Thermogravimetric analysis (TGA) of the dried powders was carried out on a TA instruments Q500 TGA analyser. Samples were heated up to 900 °C at a rate of 10 °C min⁻¹ in air, and maintained at 900 °C for 10 minutes. This enabled the actual TiO_2 content in the collected solids to be calculated.

2.5 Scale-up

The information necessary for the scale-up of production of nano- TiO_2 was consulted and agreed with the chemical engineers of plant and chemist experts of the laboratory. The precursor concentration was fixed at 0.05 M at laboratory scale, as the production of titania with this concentration is known within the group to result in high collection efficiencies with little chance of blockages. The industrial plant, with larger diameter tubing and higher flow-rates is capable of operating at higher concentrations of precursor. According to design specifications, the runs with a precursor concentration higher than 0.5 M. However, for this study the precursor concentration used in the calculations was established as 0.5 M. The increase of precursor concentration could be carried out in the future, according to working experience which

would provide further reductions in the environmental impact of CFHS and CFSS.

The scale-up has an inherent benefit over laboratory and pilot scale, due to the energy recovery. In the industrial plant a high-pressure heat exchanger recovers around 50% of energy. The outlet and inlet streams of the reactor are crossed in the heat exchanger, reducing the requirements of natural gas and associated (GHG) emissions.

For the industrial scenario, separation is carried out by sedimentation. Depending on precursor and temperature, nitric acid was needed to precipitate the nanoparticles (see Table 1). In the scale-up, sulphuric acid (H_2SO_4) was selected as acid for the same cases that needed acid solution. It has been proved in the laboratory that sulphuric acid is able to precipitate nanoparticles as well and, due to its low cost, is most likely to be used in an industrial setting.

After sedimentation, the product is washed with deionised water to remove organic and unreacted compounds, impurities, etc. A second sedimentation is carried out to remove wastewater from the washed nanoparticles. Depending on the precursor and the pH of the wastewater from the process, sodium hydroxide (NaOH) may be needed to neutralize it prior to release. The pH and quantity of NaOH necessary for neutralisation were determined by the chemical acid-base equilibrium laws. The wastewater is neutralized to a pH over 5 before purification in a water treatment plant.

In this study the boundaries establish a highly concentrated suspension of nano- TiO_2 in water as a final product. The wide range of possible applications could require suspension of nanoparticles or dried nano- TiO_2 . The last case would involve another stage such as vacuum evaporation, filtration, etc. that could be evaluated and added to our environmental assessment.

The whole process is a closed system; the precursors are dissolved in water and the reaction occurs in a closed reactor. Sedimentation uses a closed tank and results in no emissions into the air. The only emission considered is the release of nanoparticles (1%) into the wastewater before treatment in the water treatment plant (<120 mg/l). According to Honda *et al.*⁵⁰ a primary water treatment could reduce more than 90% of the concentration of nanoparticles of TiO_2 , so that after the water treatment the concentration would be lower than 12 mg/l. A recent cytotoxicity assessment was carried out as collaboration between the SHYMAN and NANOMILE projects which showed similar concentrations of TiO_2 nanoparticles have no toxic effect on HepaRG cells⁵¹. In addition, human studies conducted so far do not suggest an association between occupational exposure to titanium dioxide and an increased risk of cancer (J Prochazka, personal communication). Figure 2 shows the process flow for the industrial scale continuous flow system.

3. Results and Discussion

3.1 Phase and crystallinity

The powder X-ray diffraction patterns of the obtained materials from all syntheses are shown in Figure 3. Samples prepared from TiCl_4 show a small peak at a Bragg angle of 31° which can be attributed to brookite (ICDD 01-076-1934). A small percentage of brookite was also found by Malinger *et al.* when the pH was lower than 1 and titanium tetrachloride was used as precursor,²⁵ consistent with our own observations here. All other diffraction patterns correspond to the anatase phase of titania (ICDD 01-078-2486). A number of samples, notably those prepared from TiPO at 200 and 250 °C and TiBALD at 350 °C, also present extremely broad features centred around $30^\circ 2\theta$, which may be assigned to amorphous titania.

TEM images show that an increase in synthesis temperature results in an increase in crystallinity of the obtained nanoparticles (see Figure 6 in SI). The products from all precursors at lower temperatures are typically forming highly agglomerated clusters which prohibits accurate size determination using image analysis. Products from higher synthesis temperatures are more crystalline and typically less agglomerated.

Generally, anatase, as the kinetically favoured phase, is the expected product of rapid CFHS and CFSS conditions. The use of TiCl_4 as precursor, negatively affects the purity of the final product, due to generation of the brookite phase. Amorphous nanoparticles are produced if the reaction temperature is too low for the precursor type.

3.2 Size

The calculated crystallite diameters from the XRD analysis are shown in Figure 3(f). In all cases the crystallite sizes are calculated to be between 2.5 and 8 nm. There is a general trend towards increasing crystallite diameter with increasing temperature.

TEM images confirm similar results to the XRD; an increase in reaction temperature leads to an increase in the size of the nanoparticles (see Figure 6 in SI). TEM images and the corresponding size distributions are shown in Figure 5 for samples prepared at 400 °C from all precursors. In all cases the measured particle sizes were between 3 and 20 nm. The sample prepared from TiOS at 400 °C showed the largest mean particle size at 9.4 nm, as well as the broadest distribution. All other samples prepared at 400 °C, with the exception of those obtained from the reaction of TiBALD, exhibited mean particle sizes of between 7.5 and 8 nm. The product from TiBALD at 400 °C shows both the smallest particles and the tightest size distribution, with sizes of 6.2 ± 1.6 nm. TEM images and size distributions, where possible, of all samples are provided in the supporting information.

Malinger *et al.* synthesised nanoparticles of TiO_2 in a range of temperatures of 120-220 °C by a continuous hydrothermal process and also concluded that increasing the synthesis temperature leads an increase of size and crystallinity,²⁵ but at the expense of an increase in energy consumption. Our XRD and TEM results suggest similar conclusions i.e. higher temperatures lead bigger and more crystalline nanoparticles.

Obviously the demand of energy is higher when the temperature increases, but this affirmation should be estimated by kilogram of nano-TiO₂, because an increase of temperature could also increase the conversion of the precursors as Hobbs *et al.* demonstrated.²⁰ The use of different precursors leads to differences in the nano-TiO₂ product. A complex organic precursor like TiBALD generates small, non-agglomerated and highly crystalline nanoparticles, whilst the use of simple inorganic precursors like TiOS produce the biggest nanoparticles size and the broadest size distributions.

3.3 Yield

The solids obtained were subject to thermogravimetric analysis, as shown in Figure 4(a-e). All samples show some degree of mass loss, as would be expected, but the nature of the weight loss can be used as an indicator of downstream separation/wastewater processing issues. Samples prepared from TiOS at temperatures of 200 and 250 °C show a gradual weight loss up to ~ 130 °C due to the loss of surface bound water and hydroxides, followed by a small sharp weight loss at 330 °C which may be due to adsorbed CO₂. An additional weight loss step between 520 and 640 °C is attributed to the loss of SO₂ from residual sulphate species. Samples prepared at higher temperatures of 300, 350 and 400 °C show a faster weight loss at low temperatures from the removal of physisorbed water, while the SO₂ weight loss is significantly lessened. Samples prepared from TiCl₄ all show a sharp weight loss up to 100 °C with a further extended weight loss up to 300 °C ascribed to the loss of physisorbed and chemisorbed water and hydroxide groups, respectively. The total weight losses are typically 15 – 17%, with the exception of the sample prepared at 200 °C which loses 30% of its initial mass on heating to 900 °C. Samples prepared from TiPO all show similar thermal behaviour, with only slight weight losses of ~10% up to temperatures of 350 °C. It is worth noting that samples prepared at reaction temperatures less than 350 °C all show a weight loss, suggesting only adsorbed water (<300 °C) while those prepared at 350 and 400 °C show an additional step which is likely due to dehydroxylation. Samples prepared from both WSTCs, TiBALD and PTOOD, at temperatures of 200 – 300 °C show significant weight losses of between 28 and 47%, largely resulting from high water content and incomplete breakdown of the organic counter ion. At higher synthesis temperatures, weight losses are between just 5 and 10% and can be attributed solely to dehydration and dehydroxylation of the nanopowders. These results indicate that the increase of temperature reduces the amount of impurities in the post-reaction product, which are washed away in later stages of the process.

It is reasonably assumed that the final mass after TGA analysis is pure TiO₂. The temperature reached 900 °C, removing all organic impurities and water content. The initial mass of solid obtained after drying is adjusted according to these TGA results to ascertain an accurate conversion. The % conversion as a function of temperature is shown in Figure 4(f) for all precursors. It is generally observed that increasing the

temperature of reaction, regardless of the precursor, results in fewer impurities and a higher conversion. The sole exception to this is TiPO, which shows a significantly decreased ongoing conversion from 350 °C (93%) to 400 °C (67%). The reactions involving TiPO were carried out in IPA, the critical point of which is 235 °C and 53 bar. When the temperature of mixing in the reactor is around this point Toft *et al.* showed that the particle size could drop,⁹ while in our case it has been demonstrated that the conversion decreased. TiCl₄, which also uses IPA as a solvent, exhibits low conversion for all temperatures. This suggests that the use of IPA leads to lower conversion, relative to water. Also, the use of water is associated with a lower environmental impact than the organic solvent. The WSTC precursors (PTOOD and TiBALD) have high conversion (>70%) when the system operates above 300 °C. Of the five precursors studied only TiOS shows good conversions across all synthesis temperatures, with 100% conversion achieved above 200 °C.

The general properties and characteristics of all products are summarised in Table 1.

3.4 Cumulative Energy Demand and Global Warming Potential

Cumulative energy demand (CED) and global warming potential (GWP), quantified on a cradle-to-gate basis, vary substantially between the nano-TiO₂ production routes (Figure 6 and 7, respectively) (Table 1 and 2 SI). Generally, the precursor is found to be the main contributing factor to CED for the organic precursors, as shown in Figure 6. Also, precursors which result in low conversion and which contain organic components or solvent significantly increase the CED values. TiBALD, which is a third generation precursor (prepared from TiPO, which is itself prepared from TiCl₄), has the highest CED values, from 1952 to 6157 MJ/kg TiO₂ depending on the synthesis temperature/conversion. On the other hand, TiOS has CED values between 102 and 149 MJ/kg TiO₂. This is predominantly due to the fact that TiOS manufacturing requires fewer production steps and thus less energy. Low conversion extends production time, increasing the quantity of precursors, energy, solvents, etc. which are crucial during production. For example, using TiPO at 400 °C, with a conversion to TiO₂ of just 67%, results in a higher CED than the same precursor at other temperatures where the conversion is up to 90% (Figure 6(c)).

According to the conversion rate conclusions, it could be similarly suggested that working at higher concentrations, the energy and solvent requirements would be reduced significantly by the production of a higher quantity of product. The increase of the concentration has a clear and important limitation, i.e. potential blockages in the industrial plant. A blockage would produce a huge loss of solvents, materials, energy etc., as well as a large generation of waste.

Process chemicals also represent significant life cycle energy requirements for some nano-TiO₂ pathways. The use of the IPA as a solvent, i.e. when using TiPO and TiCl₄ precursors, contributes between 100 and 172 MJ/kg TiO₂. The bulk of this energy consumption is related to the distillation process used

to recover the isopropanol, post-production. Precursors compatible with water as solvent avoid this significant energy demand (TiOS; TiBALD; PTOOD). The use of acid to precipitate nanoparticles, as is required for all TiCl_4 preparations and several others (see Table 1) requires additional input of sulfuric acid as well as a subsequent neutralization stage and higher energy demands for wastewater treatment. For this reason the post-processing and wastewater treatment stages can make a significant contribution to CED for some nano- TiO_2 production routes. For PTOOD, acid addition is necessary for precipitation at reaction temperatures below 350 °C, contributing an additional ~80 MJ/kg TiO_2 to CED compared to production at higher temperatures that do not require acid addition.

Nano- TiO_2 production from TiOS precursor was found to have the lowest CED, ranging from 102 to 149 MJ/kg for the reaction temperatures considered in this study. This arises from a combination of a number of favourable parameters: TiOS is a “first generation” precursor with low energy requirements; it is compatible with water as a solvent; it has a conversion of ~100% when reacted at 250 °C; and does not require acid inputs for precipitation. Here the electricity, heating and cooling section is the most demanding in terms of energy. The CED increases from 53 to 100 MJ/kg TiO_2 , when the temperature goes from 250 to 400 °C. In contrast, the CED for TiPO and TiBALD is an order of magnitude larger, due primarily to the energy-intensity of precursor materials and, to a lesser extent, the use of IPA as a solvent (TiPO) and acid-assisted precipitation.

Our results indicate that nano- TiO_2 production can be achieved with similar life cycle energy expenditure as reported for micron-size TiO_2 , which range from 75 to 110 MJ/kg.^{10, 36} Given that the production of micro-size particles is comparatively less demanding, these results indicate that CFHS can be an energy-efficient means of producing nano- TiO_2 . Only the Altair process (studied by Grubb and Bakshi) was able to produce nano- TiO_2 of 40 nm, with a CED value of approximately 105 MJ/kg TiO_2 . However, the authors highlight certain omissions and incomplete data inputs⁶ and so their results may underestimate the impact of the Altair process.

The GWP of each system, as shown in Figure 7, shows similar trends as the CED analysis. Key factors impacting GHG emissions include the choice of precursor (TiPO, TiBALD, and PTOOD are associated with relatively high GWP), the use of isopropanol as a solvent, and additional process steps associated with acid-assisted precipitation. As a consequence, the TiBALD production route results in the highest GHG emissions, from 85.5 to 276.8 kg CO_2 -eq/kg TiO_2 depending on reaction temperature. On the other hand, TiOS gives the lowest emissions, of only 8.8 to 11.9 kg CO_2 -eq/kg TiO_2 . The GWP for TiPO, PTOOD and TiCl_4 range between 29 and 75 kg CO_2 -eq/kg TiO_2 depending on conversion, the use of NaOH to neutralize the effluent or the use of IPA.

The sol-gel method studied by Pini *et al.* used TiPO as the precursor for the production of 30 nm anatase nanoparticles.³⁸ The GWP impact of this process for 1 kg of TiO_2 nanoparticles is approximately of 48 kg of CO_2 -eq. With CFSS, the TiPO

precursor has emissions between 40.3 and 73.7 kg CO_2 -eq/kg of TiO_2 . This indicates that the use of both organic precursor and solvent is not as beneficial, independent of the process used.

The only reported GWP emissions similar to our results for TiOS are from the ARTS process (7.47 kg CO_2 -eq/kg TiO_2)³⁶ and traditional sulphate and chloride processes (5.31 and 6.85 kg CO_2 -eq/kg TiO_2)⁵², but they produced TiO_2 at micron-size instead of nano-size.

4. Conclusions

The production of titanium dioxide nanoparticles from five different precursors at a range of temperatures using a counter-current continuous-flow hydrothermal reactor results in anatase nanoparticles with a mean particle diameter of less than 20 nm. The precursors selected ranged from “first generation” titanium sources derived from the mining and refining of titanium ores (TiOS and TiCl_4), to more complex second (alkoxides and PTOOD) and third generation water soluble titanium complex (TiBALD).

In general, increasing the reaction temperature was found to give larger, more crystalline, nanoparticles as shown by XRD and TEM analysis. Higher synthesis temperatures also increased the purity and conversion rates. While TiOS showed the highest particle sizes and broadest size distributions, the third generation precursor TiBALD shows the smallest particle size and narrowest size distribution of samples prepared at the highest synthesis temperature. Also, the TGA results indicate that the increase in reaction temperature reduced the impurities in the post-reaction products. Samples from TiOS contained residual sulphate species, while those obtained from the WSTCs at low temperatures showed residual organics.

Life cycle assessment demonstrated that the most important factor in determining the environmental impact of the process for the production of anatase nanoparticles is the choice of precursor. Additionally, other factors that contributed to increase the environmental impact were the use of organic precursors and solvents, acid solution and the low conversion rate of some analysed routes.

Titanium oxysulphate shows the lowest environmental impacts for the production of nano- TiO_2 . It is a low-cost, first generation precursor, with few steps in its production. Its use as a precursor in the CFHS process does not necessitate the use of organic solvents, and it shows high conversion rates across a wide range of temperatures. As a result of these factors, the GWP of TiOS is between 8 and 12 kg CO_2 -eq/kg TiO_2 for all of the temperatures. CED values ranges between 100 and 150 MJ/kg TiO_2 approximately and are similarly the lowest among the precursors considered in this study. The highest impact production route is from TiBALD, due to low conversion at low reaction temperatures, the need for additional post-synthesis steps and complexity of manufacturing the precursor complex in the first place.

ARTICLE

Journal Name

Results demonstrate the potential for CFHS to achieve low environmental impacts for nanoparticle synthesis when compared with competing technologies and CFSS. Prior studies have demonstrated technical advantages of this approach, including scalability, short reaction time, high crystallinity and nano-sized production with narrow size distribution. CFHS production of nano-TiO₂ is shown to achieve similar CED and GWP compared to micro-sized particles manufactured by processes involving high temperatures and long reaction times.

In common with prior cradle-to-gate analyses of nano-TiO₂ production, care must be taken in interpreting results. Evaluation of the use of nano-TiO₂ in specific applications needs to consider the full product life cycle. Such an analysis must be informed by an understanding of the implications of nano-TiO₂ properties on environmental impacts during the use and end-of-life phases. To our knowledge, this is first time that the environmental impacts of TiO₂ production have been linked to precursor selection, process parameters, and key TiO₂ characteristics (size distribution; crystallinity). This paper therefore provides a useful foundation to future work evaluating potential applications of nano-TiO₂ and their life cycle environmental impacts.

Acknowledgements

This work is funded by the European Union's Seventh Framework Programme (FP7/2007–2013), grant agreement no. FP7-NMP4-LA-2012-280983, SHYMAN. Nigel Neate and the Advanced Materials Research Group in the Department of Mechanical, Materials and Manufacturing Engineering are gratefully acknowledged for the use of XRD and TEM facilities.

References

1. M. Cargnello, T. R. Gordon and C. B. Murray, *Chemical reviews*, 2014, **114**, 9319-9345.
2. W. Büchner, *Industrial inorganic chemistry*, VCH, 1989.
3. R. Thompson, *Industrial inorganic chemicals: production and uses*, Royal Society of Chemistry, 1995.
4. D. Macwan, P. N. Dave and S. Chaturvedi, *Journal of Materials Science*, 2011, **46**, 3669-3686.
5. Q. Li, S. Mahendra, D. Y. Lyon, L. Brunet, M. V. Liga, D. Li and P. J. Alvarez, *Water research*, 2008, **42**, 4591-4602.
6. G. F. Grubb and B. R. Bakshi, *Journal of Industrial Ecology*, 2011, **15**, 81-95.
7. B. C. Y. Chan, X. Wang, L. K. W. Lam, J. M. Gordon, D. Feuermann, C. L. Raston and H. Tong Chua, *Chemical Engineering Journal*, 2012, **211-212**, 195-199.
8. S.-i. Kawasaki, Y. Xiuyi, K. Sue, Y. Hakuta, A. Suzuki and K. Arai, *The Journal of Supercritical Fluids*, 2009, **50**, 276-282.
9. L. L. Toft, D. F. Aarup, M. Bremholm, P. Hald and B. B. Iversen, *Journal of Solid State Chemistry*, 2009, **182**, 491-495.
10. E. Reck and M. Richards, *Pigment & resin technology*, 1999, **28**, 149-157.
11. T. Adschiri, K. Kanazawa and K. Arai, *Journal of the American Ceramic Society*, 1992, **75**, 1019-1022.
12. T. Adschiri, K. Kanazawa and K. Arai, *Journal of the American Ceramic Society*, 1992, **75**, 2615-2618.
13. J. Bocquet, K. Chhor and C. Pommier, *Materials chemistry and physics*, 1999, **57**, 273-280.
14. M. Gimeno-Fabra, A. S. Munn, L. A. Stevens, T. C. Drage, D. M. Grant, R. J. Kashtiban, J. Sloan, E. Lester and R. I. Walton, *Chemical Communications*, 2012, **48**, 10642-10644.
15. E. Lester, P. Blood, J. Denyer, D. Giddings, B. Azzopardi and M. Poliakoff, *The Journal of Supercritical Fluids*, 2006, **37**, 209-214.
16. G. Aksomaityte, M. Poliakoff and E. Lester, *Chemical engineering science*, 2013, **85**, 2-10.
17. P. W. Dunne, A. S. Munn, C. L. Starkey and E. H. Lester, *Chemical Communications*, 2015, **51**, 4048-4050.
18. P. W. Dunne, C. L. Starkey, M. Gimeno-Fabra and E. H. Lester, *Nanoscale*, 2014, **6**, 2406-2418.
19. M. Gimeno-Fabra, P. Dunne, D. Grant, P. Gooden and E. Lester, *Chem. Eng. J.*, 2013, **226**, 22-29.
20. H. Hobbs, S. Briddon and E. Lester, *Green Chemistry*, 2009, **11**, 484-491.
21. E. Lester, G. Aksomaityte, J. Li, S. Gomez, J. Gonzalez-Gonzalez and M. Poliakoff, *Progress in Crystal Growth and Characterization of Materials*, 2012, **58**, 3-13.
22. E. Lester, S. V. Tang, A. Khlobystov, V. L. Rose, L. Buttery and C. J. Roberts, *CrystEngComm*, 2013, **15**, 3256-3260.
23. Q. Wang, S. V. Y. Tang, E. Lester and D. O'Hare, *Nanoscale*, 2013, **5**, 114-117.
24. J. Sierra-Pallares, T. Huddle, J. García-Serna, E. Alonso, F. Mato, I. Shvets, O. Luebben, M. J. Cocero and E. Lester, *Nano Research*, 1-11.
25. K. A. Malinger, A. Maguer, A. Thorel, A. Gaunand and J.-F. Hochepped, *Chemical engineering journal*, 2011, **174**, 445-451.
26. A. Yasin, F. Guo and G. P. Demopoulos, *Chemical Engineering Journal*, 2016, **287**, 398-409.
27. C. Pighini, D. Aymes, N. Millot and L. Saviot, *Journal of Nanoparticle Research*, 2007, **9**, 309-315.
28. N. M. Makwana, C. J. Tighe, R. I. Guar, P. F. McMillan and J. A. Darr, *Materials Science in Semiconductor Processing*, 2016, **42**, 131-137.
29. M. Chen, T. Lin, C. Y. Ma and X. Z. Wang, *Advanced Control of Chemical Processes*, 2012.
30. M. Baghbanzadeh, T. N. Glasnov and C. O. Kappe, *Journal of Flow Chemistry*, 2013, **3**, 109-113.

- 31 M. Kakihana, M. Kobayashi, K. Tomita and V. Petrykin, *Bulletin of the Chemical Society of Japan*, 2010, **83**, 1285-1308.
- 32 M. Niederberger and G. Garnweitner, *Chemistry-A European Journal*, 2006, **12**, 7282-7302.
- 33 T. Ohya, M. Ito, K. Yamada, T. Ban, Y. Ohya and Y. Takahashi, *Journal of sol-gel science and technology*, 2004, **30**, 71-81.
- 34 F. Brisse and M. Haddad, *Inorganica Chimica Acta*, 1977, **24**, 173-177.
- 35 V. G. Kessler, *Journal of sol-gel science and technology*, 2013, **68**, 464-470.
- 36 S. Middlemas, Z. Z. Fang and P. Fan, *Journal of Cleaner Production*, 2015, **89**, 137-147.
- 37 S. Middlemas, Z. Z. Fang and P. Fan, *Hydrometallurgy*, 2013, **131**, 107-113.
- 38 M. Pini, R. Rosa, P. Neri, F. Bondioli and A. M. Ferrari, *Green Chemistry*, 2015, **17**, 518-531.
- 39 T. SHYMAN-project, *Website SHYMAN Project: <http://www.shyman.eu/project.php>*, [Accessed 1 Sept. 2015].
- 40 ISO-14040, *Environmental management - Life cycle assessment - Principles and framework*, 2006.
- 41 ISO-14044, *Environmental management - Life cycle assessment - Requirements and guidelines*, 2006.
- 42 V. Katari, T. W. Devitt and T. Parsons, 1977.
- 43 C. Baroch, T. Kaczmarek, W. Barnes, L. Galloway, W. Mark and G. Lee, *TITANIUM PLANT AT BOULDER CITY, NEV.: ITS DESIGN AND OPERATION*, Bureau of Mines, 1955.
- 44 F. Francesco, S. Renzo and S. Giuseppe, Google Patents, 1971.
- 45 J. Nelles, Google Patents, 1940.
- 46 D. Bradley, D. Hancock and W. Wardlaw, *Journal of the Chemical Society (Resumed)*, 1952, 2773-2778.
- 47 D. Bradley, R. Mehrotra and W. Wardlaw, *Journal of the Chemical Society (Resumed)*, 1952, 2027-2032.
- 48 G. Van de Velde, S. Harkema and P. Gellings, *Inorganica Chimica Acta*, 1974, **11**, 243-252.
- 49 J. M. Sullivan, J. W. Williard, D. L. White and Y. K. Kim, *Industrial & engineering chemistry product research and development*, 1983, **22**, 699-709.
- 50 R. J. Honda, V. Keene, L. Daniels and S. L. Walker, *Environmental engineering science*, 2014, **31**, 127-134.
- 51 Nanomile, *Nanosafety Cluster Compendium 2016*, <http://nanomile.eu-vri.eu/filehandler.ashx?file=15553>.
- 52 B. P. Weidema, C. Bauer, R. Hischier, C. Mutel, T. Nemecek, J. Reinhard, C. Vadenbo and G. Wernet, *Overview and methodology: Data quality guideline for the ecoinvent database version 3*, Swiss Centre for Life Cycle Inventories, 2013.

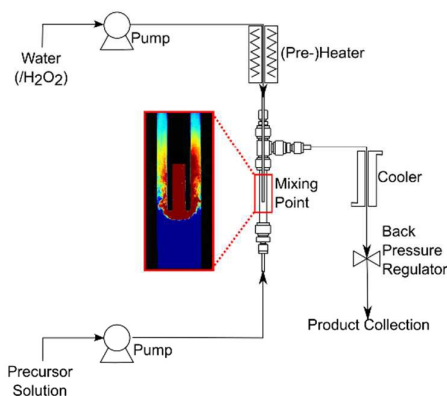


Figure 1. Simplified schematic of the counter-current continuous-flow hydrothermal reactor.

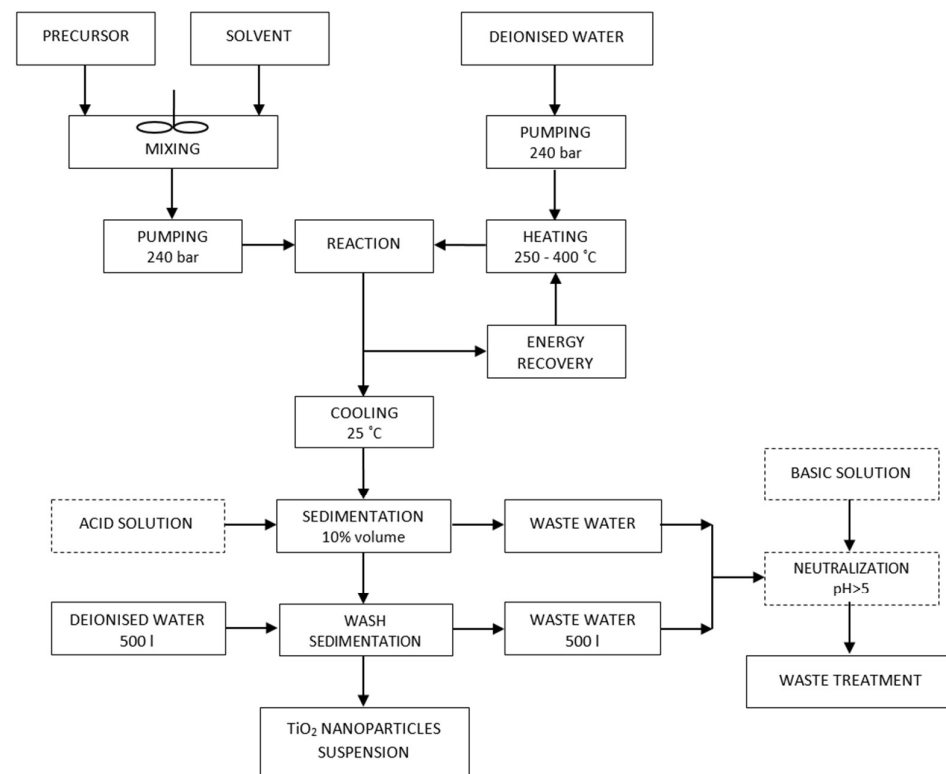


Figure 2. Scheme for the large scale continuous-flow production of titania nanoparticles.

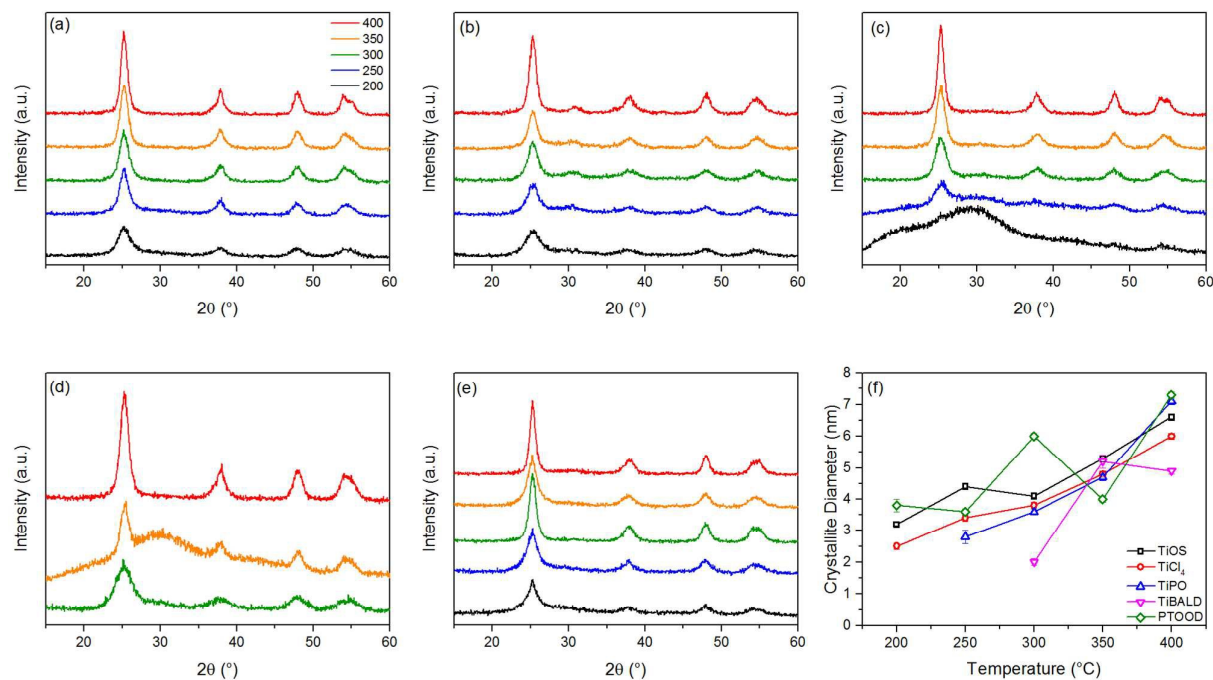


Figure 3. Powder X-ray diffraction patterns of products obtained at varying reaction temperatures from five different precursors: a) titanium oxysulfate, b) titanium tetrachloride, c) titanium isopropoxide, d) titanium bis(ammonium lactato) dihydroxide and e) potassium titanium oxide oxalate; and f) the corresponding calculated crystallite diameters.

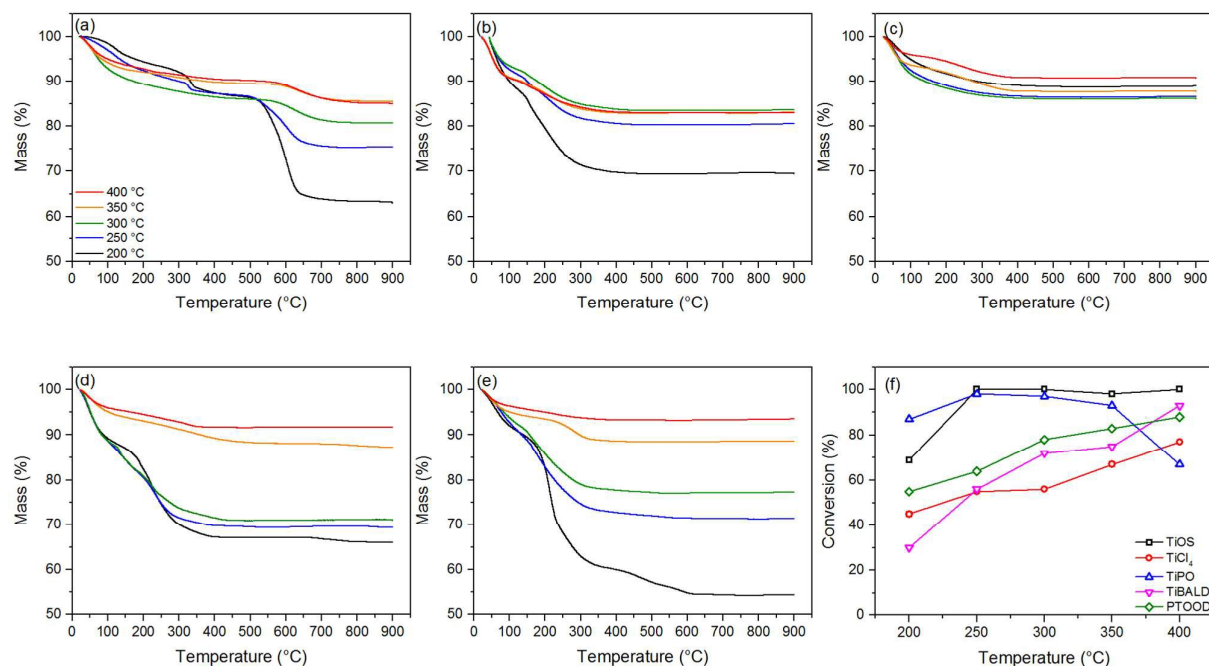


Figure 4. Thermogravimetric traces of products obtained at varying reaction temperatures from five different precursors: a) titanium oxysulfate, b) titanium tetrachloride, c) titanium isopropoxide, d) titanium bis(ammonium lactato) dihydroxide and e) potassium titanium oxide oxalate; and f) the % conversion for each synthesis.

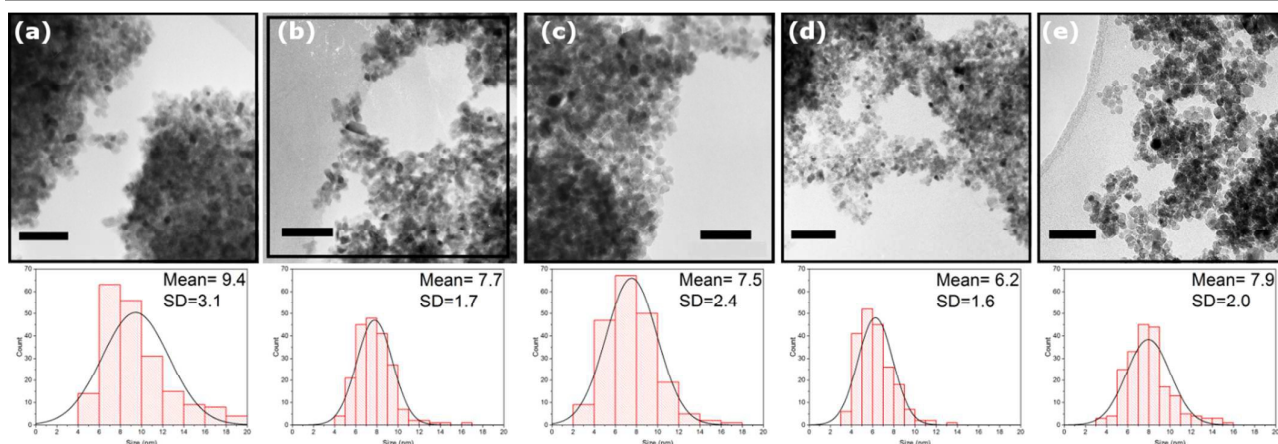


Figure 5. TEM images and corresponding size distributions (n = 200) of samples prepared at 400 °C from a) titanium oxysulfate, b) titanium tetrachloride, c) titanium isopropoxide, d) titanium bis(ammonium lactato) dihydroxide and e) potassium titanium oxide oxalate. Scale bars represent 50 nm.

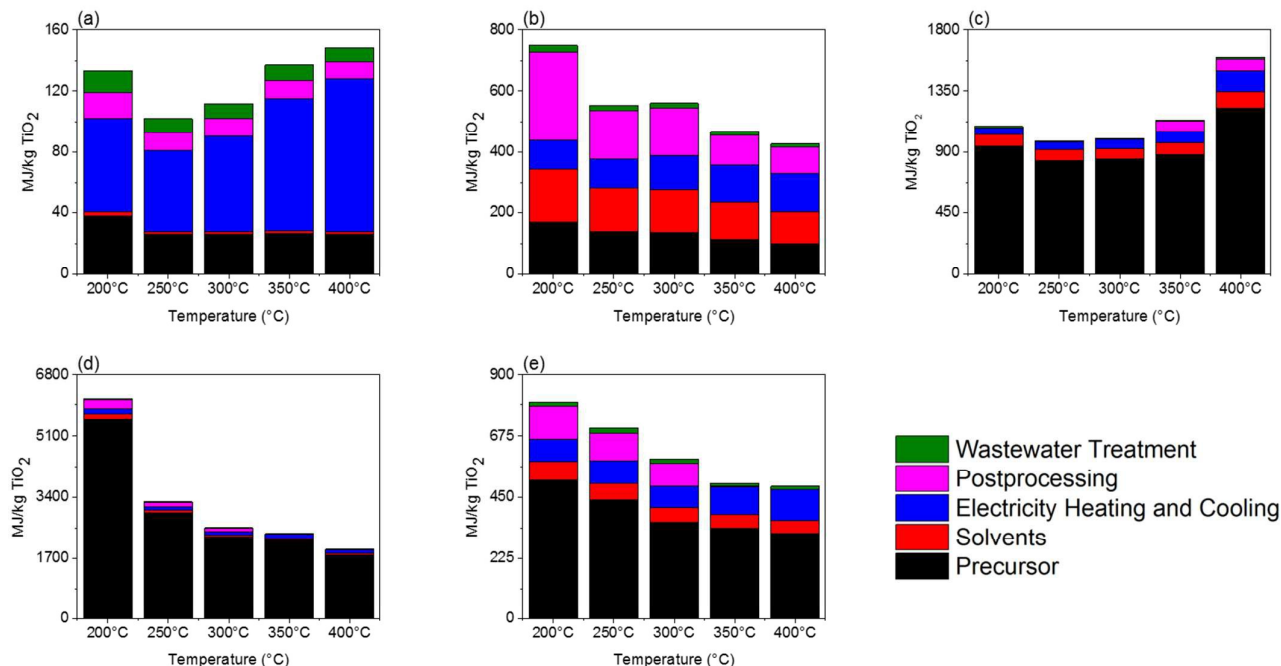


Figure 6. The cumulative energy demand (CED) to produce 1 kg of titania nanoparticles at each synthesis temperature from: a) titanium oxysulfate b) titanium tetrachloride, c) titanium isopropoxide, d) titanium bis(ammonium lactato) dihydroxide and e) potassium titanium oxide oxalate.

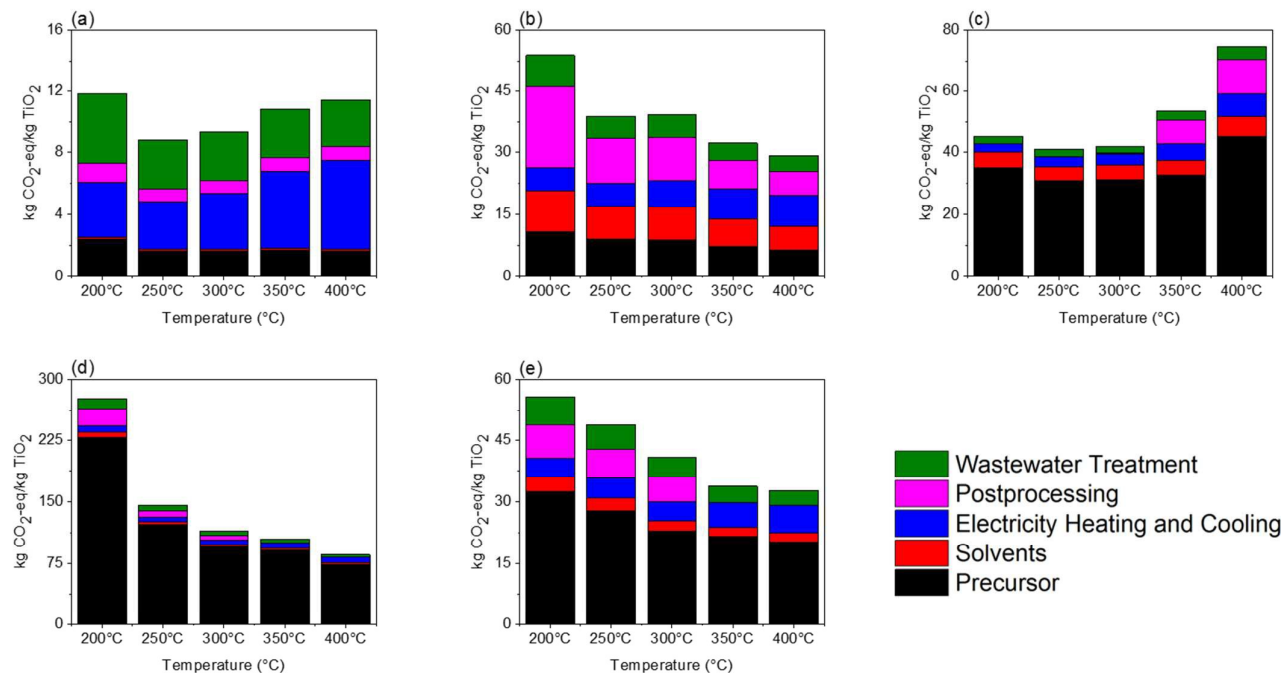


Figure 7. The global warming potential (GWP) to produce 1 kg of titania nanoparticles at each synthesis temperature from: a) titanium oxysulfate b) titanium tetrachloride, c) titanium isopropoxide, d) titanium bis(ammonium lactato) dihydroxide and e) potassium titanium oxide oxalate.

Table 1. Summary of the properties of products obtained from the lab-scale continuous flow synthesis of titania nanoparticles. An. = anatase, B. = brookite, Am. = amorphous.

Precursor	Type of Synthesis	Temperature (°C)	Precipitant	Phase	Weight Loss (%)	Conversion (%)	XRD Size (nm)	TEM Size (nm)
TiOS	Hydrothermal	200		An.	37	69	3.2	-
		250		An.	24.5	100	4.4	-
		300		An.	19.3	100	4.1	5.1 ±1.4
		350		An.	14.5	98	5.3	6.1 ±1.7
		400		An.	15.0	100	6.6	9.4 ±3.1
TiCl ₄	Solvothermal	200	✓	An.	30.6	45	2.5	-
		250	✓	An.	16.9	55	3.4	-
		300	✓	An./ B.	16.3	56	3.8	6.2±1.3
		350	✓	An./ B.	16.9	67	4.8	6.6±2.2
		400	✓	An./ B.	17	77	6.0	7.7±1.6
TiPO	Solvothermal	200		Am.	10.6	87	-	-
		250		An./ Am.	11.5	98	2.8	-
		300		An.	11.9	97	3.6	4.7±1.3
		350	✓	An.	10.5	93	4.7	6.5±1.8
		400	✓	An.	8.8	67	7.1	7.5±2.4
TiBALD	Hydrothermal	200	✓	An./ Am.	34	30	-	-
		250	✓	An./ Am.	30.6	56	-	-
		300	✓	An.	29	72	2.0	6.2±1.8
		350		An.	12.8	75	5.2	-
		400		An.	8.3	93	4.9	6.2±1.6
PTOOD	Hydrothermal	200	✓	An./ Am.	45.5	55	3.8	-
		250	✓	An.	28.5	64	3.6	-
		300	✓	An.	23	78	6.0	7.5±2.1
		350		An.	11.5	83	4.0	5.8±1.5
		400		An.	6.5	88	7.3	7.9±2.0